

Experimental tests for evaluating the stability of a new nano-silica based protective for Sperone stone in comparison to traditional products

Cite as: AIP Conference Proceedings **2257**, 020012 (2020); <https://doi.org/10.1063/5.0023721>
Published Online: 03 September 2020

C. Pelosi, L. Lanteri, G. Agresti, et al.



View Online



Export Citation

ARTICLES YOU MAY BE INTERESTED IN

[Corrosion behavior of Cu-Zn-Al shape memory alloy in controlled environments](#)

AIP Conference Proceedings **2257**, 020013 (2020); <https://doi.org/10.1063/5.0024692>

[Gold nanoparticles-based extraction of phenolic compounds from olive mill wastewater: A rapid and sustainable method](#)

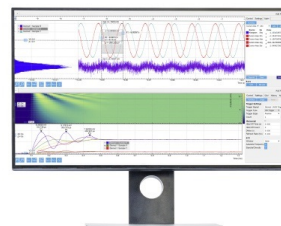
AIP Conference Proceedings **2257**, 020010 (2020); <https://doi.org/10.1063/5.0023606>

[Engineering the optical reflectance of randomly arranged self-assembled semiconductor nanowires](#)

AIP Conference Proceedings **2257**, 020009 (2020); <https://doi.org/10.1063/5.0023675>

Challenge us.

What are your needs for
periodic signal detection?



Zurich
Instruments



Experimental Tests for Evaluating the Stability of a New Nano-silica Based Protective for Sperone Stone in Comparison to Traditional Products

C. Pelosi^{1, a)}, L. Lanteri¹, G. Agresti¹, G. Rubino¹, F. Persia², G. Bonifazi³, S. Serranti³, G. Capobianco³

¹*University of Tuscia, Department DEIM, Largo dell'Università, 01100 Viterbo (Italy)*

²*ENEA Centro Ricerche Casaccia, Laboratory of Chemical and physical technologies, Via Anguillarese, 301 00123 Santa Maria di Galeria RM (Italy)*

³*Sapienza University of Rome, Department DICMA, Via Eudossiana Via Eudossiana 18, 00184 Rome (Italy)*

^{a)}Corresponding author: pelosi@unitus.it

Abstract. This paper reports the results of a preliminary investigation aimed at testing the stability of a new functionalized nano-silica based protective, named Silo N7, in comparison to traditional commercial products, i.e. polysiloxane and fluorinated elastomer. The product has been applied on an igneous rock known as Sperone stone, widely used in the south-east area of Rome, where the rock is mainly quarried. The work was performed within the activities of the ADAMO project as part of the Center of Excellence Technological District of Cultural Heritage of Lazio Region. The choice of the protective products and of the most suitable tests was made according to the standards UNI EN17114:2019 and UNI EN16581:2016 respectively. Colour measurements, contact angle evaluation, capillarity adsorption and hyperspectral imaging were performed to evaluate the performance of the chosen products.

INTRODUCTION

The aim of the work has been to investigate the behaviour of three protective products applied on the Sperone stone used for the construction of the fountains in Villa Mondragone, located southeast of Rome, in the municipality of Monte Porzio Catone, one of the site selected for the activities of ADAMO project. ADAMO (Analysis, Diagnostics and Monitoring of Cultural Heritage, <http://progettoadamo.enea.it/>) is a project of the Center of Excellence of Technological District for Cultural Heritage of Lazio Region, which includes the five Universities of Lazio, and the Italian research organisms CNR, ENEA and INFN (see more information at the website: <https://dtclazio.it/>).

Villa Mondragone is a grandiose building of approximately 8000m² plant based on four levels [1]. It is located on the Colli Laziali or Colli Albani, an ancient volcanic system southeast of Rome. Its early construction was started more than four centuries ago, while the building of the modern part of the villa can be dated back to the first century a.D. The Renaissance villa, in fact, was constructed on the Roman *Villa dei Quintili* whose remains are still visible today under the modern structure [2,3].

The gardens of the Renaissance villa are characterized by some beautiful fountains made of Sperone stone, a deposit of welded volcanic scoriae forming a portion of the Tuscolanio-Artemisio caldera rim, set near the town of Tuscolo (Fig. 1) [4,5].

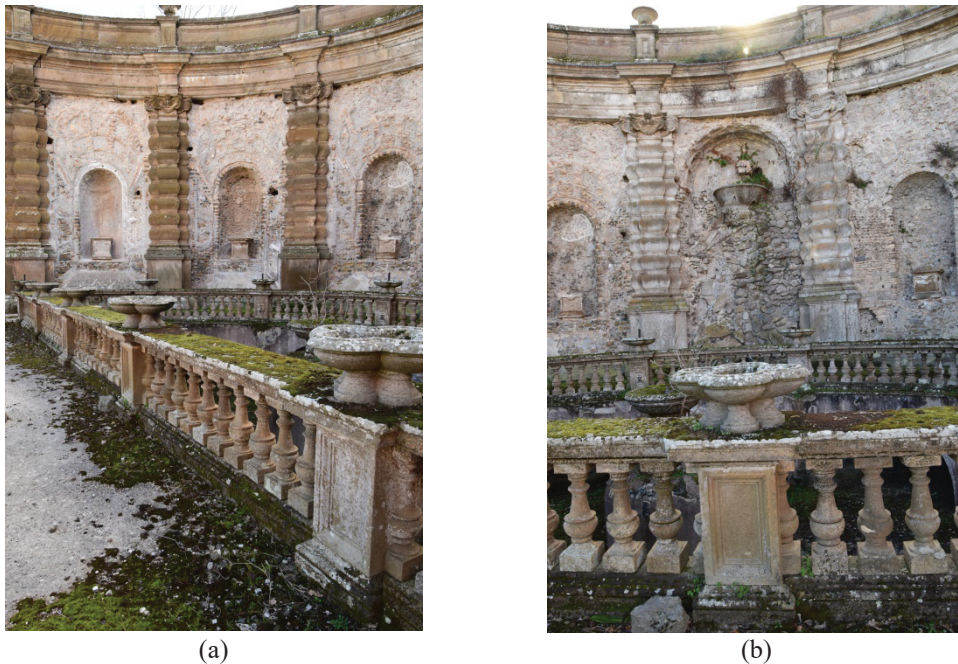


FIGURE 1. Two views of the fountain of Girandola in the right side of the villa garden. The samples of Sperone stone were obtained from rather large erratic fragments near that fountain.

The samples of Sperone stone, necessary for the laboratory test, were obtained from erratic blocks collected in the area of the fountain of Girandola. Three protective products were selected on the basis of literature data, interviews to professional restores, skilled in the restoration of stone artworks and surfaces, and of the indications given by the European standard [6]. The most used products for the protection and hydrophobicity increase of tuff rocks are poly-siloxane based formulates applied both in water and organic solution [7-9]. Another class of commercial products used in stone protection with hydrophobicity increase property, is the fluorinated elastomers applied in water dispersion [10] or solution [7]. Different kinds of emulsions with nano-structured materials have also been tested for yellow and grey tuffs and for other types of stone [8,11-15].

The behaviour of the chosen protective products was tested by following the recommendations supplied in the UNI EN16581:2016 [16]. Colour, contact angle, capillarity adsorption and hyperspectral imaging were chosen as methods for testing the performance of the protective before and after artificial ageing tests carried out under simulated solar irradiation and thermo-hygrometric cycles.

MATERIALS AND METHODS

Blocks of Sperone stone, taken from the fountain of Villa Mondragone, were cut with a diamond blade in order to obtain 5 cm x 5 cm x 2.5 cm samples according to the standards UNI EN. In order to obtain regular surfaces and to satisfy the requirements for subsequent protective application, samples were sanded with 180 grit size sandpaper. Before applying the protective products, the stone samples were dried in a laboratory oven at 60 °C until they reached constant weight.

The commercial protective products selected for the experimental tests were: Rhodorsil H224 a poly-siloxane based polymer and Fluoline HY a fluorinated copolymer. Moreover a new product supplied by CTS for the present work with the name of Silo N7 but not yet in commerce at the moment of the experimental, was tested. This last protective product is a functionalized nano-silica, according to the information supplied by CTS. The characteristics of each protective and the detailed procedures used for their application are shown in Table 1, as derived from the technical data sheets supplied with the products. After the protective application, samples were left at room temperature for thirteen days in order to let the solvent evaporate, again according to the indication supplied with the technical data sheets and by the EN standards. The weight of each sample was monitored until constant value.

TABLE 1. Product characteristics and application procedure, according to the technical data sheets from the supplier.

Chemical-physical characteristics and application	Silo N7	Rhodorsil H224	Fluoline HY
Composition	Functionalized nano-silica	Alkyl poly-siloxane	Fluorinated copolymer
Solvent	Water	Aliphatic hydrocarbons	Acetone/butyl acetate
Physical state	Liquid	Liquid	Liquid
Colour	White	Colourless or slightly yellow	Colourless
Viscosity	1 mPa·s at 20 °C	20 mm ² /s at 25 °C	20-100 cP (Brookfield)
Applied mixture	1:1 v/v in demineralized water	6% v/v in white spirit	Without dilution
Method of application	Brush	Brush	Brush
Number of treatments	2 (consecutive)	2 (the 2 nd after 3 days)	2 (the 2 nd after 3 days)
Number of samples	8	8	8

Samples were aged under two different conditions: 1) in a Solar Box chamber model 1500E by Erichsen Instruments, equipped with a 2.5 kW xenon-arc lamp and UV filter that cuts off the spectrum at 280 nm, for 1000h at 55 °C and 550 W/m², 2) in a climatic chamber Angelantoni for 15 cycles; each cycle lasted 12 hours: 1 hour for reaching T=60 °C and RH=90%, 10 hours under these conditions, then 1 hour for returning to T=20 °C and RH=30%.

Colour was measured before and after the application of the products in order to evaluate the changes caused to the stone due to their presence, and before and after ageing to detect possible variations caused by solar irradiation and thermo-hygrometric stress. An X-Rite CA22 reflectance spectrophotometer operating in the visible range was used, according to the CIELAB1976 colour system, where L* describes the lightness while a* and b* describe the chromatic coordinates on the green-red and blue-yellow axes, respectively. The characteristics of the colour measuring instrument are the following: colour scale CIEL*a*b*; illuminant D65; standard observer 10°; geometry of measurement 45°/0°; spectral range 400–700 nm; spectral resolution 10 nm; measurement diameter 4mm. Before taking measurements, the instrument was calibrated with the white reference tile (calibration reference DTP22–62 A013335) supplied by X-Rite, that is a 1 cm × 1 cm white ceramic tile. The differences in lightness (ΔL^*), chromatic coordinates (Δa^* and Δb^*), and total colour (ΔE^*) were then calculated using these parameters according to UNI EN15886 [17]. The total colour difference, ΔE^* , between two measurements (L^*_1, a^*_1, b^*_1 and L^*_2, a^*_2, b^*_2) is the geometrical distance between their positions in CIELAB colour space. It is calculated using the following equation: $\Delta E^*_{2,1} = [(\Delta L^*)^2 + (\Delta a^*)^2 + (\Delta b^*)^2]^{1/2}$. Due to the inhomogeneity of the stone, 15 measurements were performed on each 5 cm x 5 cm x 2.5 cm sample.

Capillarity adsorption test and contact angle measurements were performed before and after artificial ageing in Solar Box order to evaluate the effect of the protective ageing on the hydrophobicity of the surfaces. The capillarity adsorption test and the contact angle determination were carried out on the base of standards UNI EN15801 [18] and UNI EN15802 [19], respectively. Specifically, the values of contact angle were obtained by measuring the angle, in the liquid phase, generated by the tangent to water drop profile and the stone solid surface. The measurement was performed by observing the drop through a FireWire camera with telecentric optics and 55 mm focus length. The measurements were taken from 0 s to 60 s: the software OneAttension elaborated directly the visual data supplying the values of contact angles every 0.07 s.

Hyperspectral imaging (HSI) was performed before and after the simulated solar irradiation tests in the wavelength interval 1000-2500 nm (SWIR). The investigations were developed with Specim SISUChem XL™, embedding an ImSpector™ N25E (Specim Ltd, Finland) acting in the range from 1000 to 2500 nm, with a spectral sampling/pixel of 6.3 nm, coupled with a MCT camera (320 x 240 pixels). Pixel resolution was 14 bits. Other specific information about the technique set-up, the acquisition, and the calibration has been widely described in previous papers [20-24]. Spectral analysis of HSI derived data was carried out by adopting standard chemometric methods, with the PLS_Toolbox (Version 8.2 Eigenvector Research, Inc.) running inside Matlab (Version 8.4, The Mathworks, Inc.) [25-30]. Principal Component Analysis (PCA) was applied as a powerful and versatile method capable of providing an overview of complex multivariate data. PCA can be used for revealing relations existing between variables and samples [31]. To evaluate the variance of all samples both at 0 hours (T0) and 1000 hours (T1000) of ageing, the data were concatenated in a single mosaic hypercube as shown in Fig. 2.

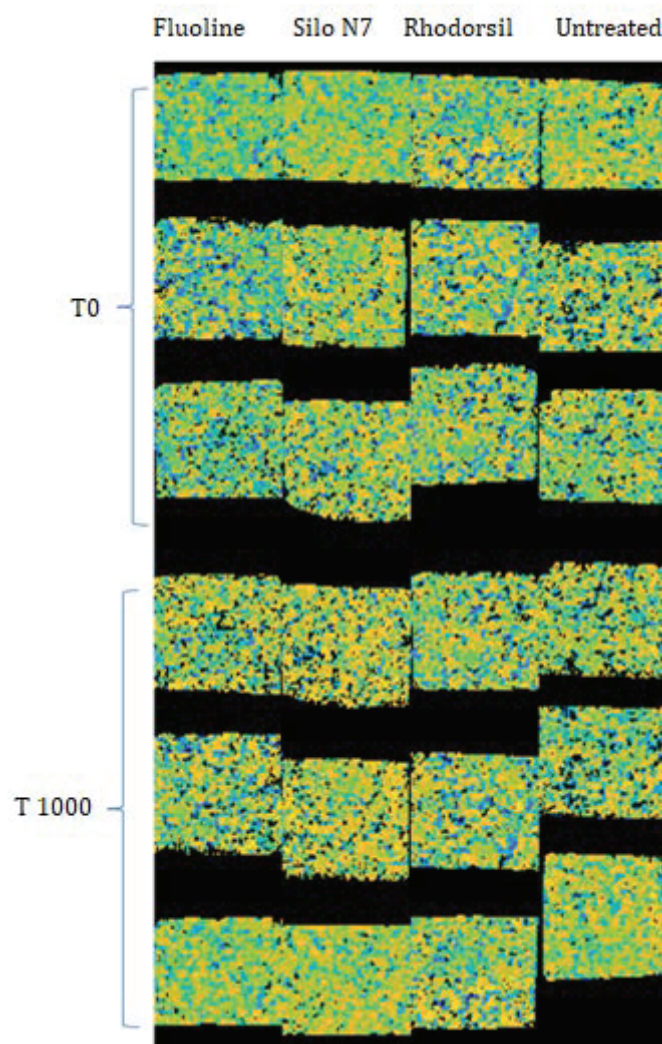


FIGURE 2. Mosaic hypercube of samples analysed at T=0h and T=1000h with different treatments (Fluoline HY, Silo N7, Rhodorsil H224, untreated). The colours are representative of sample surface reflectance values as resulting after background removal. The lighter is the colour the highest is sample surface reflectance response.

RESULTS AND DISCUSSION

The first obtained results concern the weight and colour changes caused by the application of the three selected products. In regards to the weight variation, the samples treated with Silo N7 had a variation of 0.18 ± 0.02 g, those treated with Rhodorsil H224 of 0.07 ± 0.01 g and those with Fluoline HY of 0.10 ± 0.06 g. From these data it can be derived that the highest quantity of product absorbed by the stone is Silo N7. This is probably due to its composition based on nano-silica and on the presence of water as a solvent that clearly penetrates easily in the stone due to the chemical affinity, causing higher protective accumulation.

A further interesting result concerns the colour changes that can be appreciated also by eye (Fig. 3) and that are mainly associated to a darkening of the stone. The chromatic changes, expressed as differences of L^* , a^* , b^* , and total colour change (ΔE) are reported in Table 2.

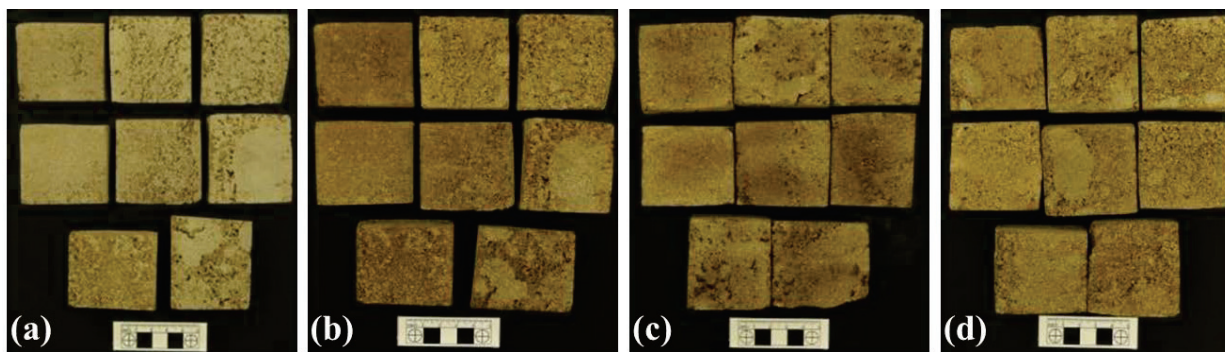


FIGURE 3. Photographs of the samples untreated (a) and treated with the selected protective products: (b) Silo N7, (c) Rhodorsil H224 and (d) Fluoline HY.

TABLE 2. Chromatic changes of the colour coordinates and ΔE as a consequence of the application of the protective products.

Sample treatment	ΔL^*	Δa^*	Δb^*	ΔE
Silo N7	-9.15	2.29	3.24	9.97
Rhodorsil H224	-12.0	3.21	4.26	13.1
Fluoline HY	-8.90	2.69	3.59	9.97

From the data of Table 2 is evident that in all cases the products cause significant differences in the surface of the Sperone stone. The main changes is calculated for L^* coordinate (representing lightness) that undergoes a significant decrease (darkening of the surfaces). Rhodorsil H224 represents the protective product that causes the most relevant stone variation in colour. Colour variations were calculated also before and after ageing tests both in Solar Box chamber, simulating solar irradiation, and in climatic chamber, simulating thermo-hygrometric cycles.

Also in this case differences of the chromatic coordinates L^* , a^* and b^* , and ΔE were calculated, the results are reported in Table 3. The data of Table 3 show the high stability of protective products, in fact the changes of colour are low, certainly below the limit perceptible by the human eye, both for samples aged in under thermo-hygrometric stress and under simulated solar radiation. This result demonstrated the stability of the protective products in terms of colour variations caused by artificial ageing processes.

According to the standard UNI EN16581, a capillarity absorption test was performed before and after ageing in the Solar Box chamber in order to evaluate the possible changes caused by the irradiation on the performance of the protective products. The overall results are reported in Table 4. The values in the table are the quantities of water absorbed by the samples on the area exposed to the imbibed filter paper, according to the standard UNI EN15801.

The equation used for obtaining these values is: $Q_i = \frac{m_i - m_0}{A} \times 1000$, where m_i (g) is the weight of the wet sample at time t_i (\sqrt{s}), m_0 (g) is the weight of the dry sample and A (cm^2) is the area of the sample in contact with the filter paper imbibed of demineralized water.

The data in Table 1 highlight that, as expected, the untreated samples absorb rapidly the water and reach saturation in a short time. On the other hand, samples treated with Rhodorsil H224, before ageing, absorb little quantities of water and the protective seems to well act as a hydro-repellent product.

TABLE 3. Chromatic changes of the colour coordinates and ΔE as a consequence of ageing of the samples.

Sample treatment	ΔL^*	Δa^*	Δb^*	ΔE
AGEING IN CLIMATIC CHAMBER				
Untreated	0.949	-0.233	-0.466	1.80
Silo N7	1.787	-0.447	-0.829	2.02
Rhodorsil H224	1.109	-0.105	0.197	1.13
Fluoline HY	0.898	-0.299	-0.372	1.02
AGEING IN SOLAR BOX CHAMBER				
Untreated	0.866	0.195	0.121	0.895
Silo N7	3.18	-0.867	-1.71	3.71
Rhodorsil H224	0.768	-0.087	-0.037	0.774
Fluoline HY	1.53	-0.389	-0.542	1.67

In the cases of samples treated with Silo N7 and Fluoline HY, before ageing in Solar Box, the water absorption is low in the early measurements, but over a longer period of time, it increase reaching values similar to those obtained for the untreated samples, apart for sample S1, treated with Silo N7, that exhibits low capillarity absorption values at all times. These results may be explained if considering the highly heterogeneity of Sperone stone and the presence of cracking phenomena due to the long exposure of the samples to environmental agents (for what concerns the samples taken from the garden of Villa Mondragone). In fact, sample S1 is homogeneous and this could explain the different behaviour in respect to the other ones.

The water absorption measurements after ageing in Solar Box chamber show similar trends to those found before ageing. However, the values obtained after ageing are generally higher than those reckoned before irradiation. This result can be explained considering that the absorbed water in the test conducted before ageing, had a cleaning action in the stone's pores so favouring its absorption during the test after ageing.

The effect of protective treatment on Sperone stone samples had been evaluated by measuring the contact angle that, in respect to capillarity absorption test, can be considered a punctual measurement as it interests the areas where the drop is placed only. For this reason, contact angle measurements were performed on five points on each sample. The results of contact angle measurements and the calculated average values are reported in Table 5. They were obtained before and after artificial ageing in the Solar Box chamber. The contact angle test is very significant for evaluating the effectiveness of the applied protective. In fact, the behaviour of the drop placed both on the treated and untreated samples, is completely different. Untreated samples don't show any contact angle value, as the drop disappears immediately. While, in some cases the drop seems to bounce off the surface of the treated samples. By comparing the data of each sample treated at time $t=10s$ and at time $t=60s$, it is noted that for the same measurement the value of the contact angle is almost constant. This means that the drop remained stable over the 60 seconds of the test, i.e. the protective products have an effective water-repellent action. Among all, the protective that gives the material less wettability, in the test prior to the aging process, is Rhodorsil H224. The samples treated with this product are characterized by a contact angle value close to 180° which represents the wettability condition equal to zero. Analyzing the data obtained from the measurements of the contact angle after the aging process, it is noted, also in this case, that the protective products effectively retain the drop, hindering the penetration into the material. The overall results of the contact angle measurement, allow for assessing that in all cases the protective guarantee high hydrophobicity of the stone surfaces and that the ageing under simulated solar radiation doesn't significantly affect the behaviour of the products.

The last technique applied within the ADAMO project to test the performance of the protective treatments, is the Hyperspectral Imaging (HSI) in the short wave infrared (SWIR) region of the electromagnetic spectrum, which demonstrated a powerful non-invasive method for obtaining also predictive models for investigating the effect of ageing on treated samples in cultural heritage application [20-24, 32, 33].

TABLE 4. Results of capillarity absorption test in terms of absorbed water as function of time expressed in s^{1/2}.

Sample	$\sqrt{t} \text{ (s}^{1/2}\text{)}$									
	24.49	34.64	42.43	60.00	120.00	146.97	293.94	415.69	509.12	587.88
BEFORE AGEING IN SOLAR BOX CHAMBER										
Untreated (S25)	374.8	379.2	376.0	380.4	388.0	381.6	371.6	426.4	421.2	457.2
Untreated (S26)	422.0	439.6	431.2	441.6	438.0	435.6	426.8	468.4	487.2	507.6
Untreated (S27)	399.2	444.0	443.2	451.2	442.0	445.6	418.0	451.6	494.8	535.2
Silo N7 (S1)	5.200	7.600	9.000	12.40	20.40	23.20	32.00	37.20	42.00	46.00
Silo N7 (S2)	6.000	8.800	11.60	94.80	382.0	392.0	418.8	448.4	486.4	501.2
Silo N7 (S3)	6.800	10.00	12.80	22.80	372.4	384.8	414.0	428.4	461.6	487.6
Rhodorsil H224 (S9)	6.000	23.60	24.80	27.20	32.80	34.40	42.00	47.20	51.60	54.40
Rhodorsil H224 (S10)	5.200	8.000	8.800	12.80	20.40	22.80	30.80	34.80	37.60	39.60
Rhodorsil H224 (S11)	5.200	7.600	9.600	12.80	20.40	23.60	32.80	37.60	41.60	44.80
Fluoline HY (S17)	4.400	7.200	9.200	12.40	20.40	22.80	34.40	42.40	382.4	408.4
Fluoline HY (S18)	6.000	47.20	90.00	194.8	431.2	435.2	451.6	484.0	518.4	528.4
Fluoline HY (S19)	6.000	28.40	30.00	31.60	38.40	40.40	434.8	462.8	501.6	510.4
AFTER AGEING IN SOLAR BOX CHAMBER										
Untreated (S25)	374.0	375.6	378.0	389.2	351.6	370.0	567.6	442.8	439.2	422.8
Untreated (S26)	411.2	407.2	426.8	420.4	401.2	422.4	468.0	500.4	489.6	511.6
Untreated (S27)	413.6	412.4	437.2	431.6	367.6	425.2	481.6	507.6	518.8	502.0
Silo N7 (S1)	3.600	6.800	8.400	12.00	20.00	23.20	30.40	38.00	56.40	58.80
Silo N7 (S2)	132.4	263.6	358.8	380.0	399.2	414.8	452.0	482.0	481.2	499.2
Silo N7 (S3)	291.6	368.8	375.2	389.6	392.8	416.0	460.8	471.2	481.6	502.0
Rhodorsil H224 (S9)	3.600	6.400	7.200	12.40	22.80	27.20	34.00	415.6	442.8	463.2
Rhodorsil H224 (S10)	3.200	5.200	6.400	9.200	17.20	21.60	28.40	32.40	36.00	54.00
Rhodorsil H224 (S11)	4.000	7.600	7.600	11.20	138.8	253.2	364.0	396.8	409.2	424.4
Fluoline HY (S17)	149.2	256.6	325.6	350.8	351.2	352.4	396.4	417.2	420.8	434.0
Fluoline HY (S18)	357.6	411.6	416.0	410.4	416.4	422.4	476.8	506.0	505.2	504.8
Fluoline HY (S19)	412.0	414.4	406.0	418.8	412.8	417.6	464.0	491.2	502.0	510.4

In Fig. 4 the results for all investigated samples are reported as PCA score plot and mosaic of the data acquired through HSI. PCA score plot have been computed starting from the collected spectra as resulting from preprocessing based on sequential application of the following algorithms: Standard Normal Variate (SNV), Smoothing, Detrend and Mean Centering (MC). The PCA model shown in Fig. 4 highlights the spectral variation between the treated and untreated samples. The PCA score density plots allow calculating the number of pixels with identical scores.

More in the detail, the colour code scale highlights the higher density of pixels in the point clouds. The PCA model was composed of three principal components (PCs) showing a total captured variance of 90.54%, i.e. 63.10% of PC1, 16.82% of PC2 and 10.62% of PC3. PC1 and PC3 mainly highlight the variance relative to the common matrix analysed (e.g. Sperone Stone), while PC2 highlights the spectral difference between the untreated and the treated samples. The PCA score plots in Figure 4 (and the corresponding loadings plots) show how PC1 vs PC2 and PC2 vs PC3 highlight 2 distinct clouds. The higher density cloud characterizes the treated samples while the lower density cloud characterizes the untreated samples. The PCA does not show significant variations in respect of the aging time (i.e. T=0h and T=1000h). The positive values of PC1 are mainly due to the spectral region from 1400 nm to 2100 nm, while the regions from 1000 nm to 1400 nm and from 2200 nm to 2500 nm mainly influence the variance of the negative PC1. Positive PC2 values are mainly due to variance in regions from 1300 nm to 1500 nm and from 1900 nm to 2200 nm, while the negative values of PC2 are mainly due to the variance in the regions from 1000 nm to 1300 nm, from 1500 nm to 1900 nm and from 2200 nm to 2500 nm. The positive values of PC3 are mainly due to the variance in the region from 1000 nm to 1200 nm, while the negative values of PC3 are mainly due to the variance in the regions from 1200 nm to 1600 nm. In conclusion, PCA clearly shows that there is spectral difference between treated and untreated samples, confirming the presence of the protective layer on the surfaces of all examined samples. PCA also highlights that there is no evident difference between samples before and after 1000h of ageing in the Solar Box chamber. The overall result shows an unbalanced separation with an asymmetric data variance. In detail the variance was more influenced by the greater population of treated samples compared to the untreated samples. For this reason, in order to maximize the variance for each protective, the data were analysed separately for each treatment (Figs. 5-8).

TABLE 5. Contact angles values measured before and after the ageing of the samples in Solar Box chamber.

	Measure 1	Measure 2	Measure 3	Measure 4	Measure 5	Average Value
BEFORE AGEING						
Silo N7 t=10s	149.02	144.31	145.66	149.26	125.02	142.65
Silo N7 t=60s	148.62	141.74	145.24	148.61	124.26	141.69
Rhodorsil H224 t=10s	142.45	161.49	157.09	157.79	166.62	157.09
Rhodorsil H224 t=60s	142.17	160.94	156.46	157.07	164.36	156.20
Fluoline HY t=10s	138.56	130.61	134.42	139.22	142.43	137.05
Fluoline HY t=60s	138.82	130.02	133.68	138.42	141.76	135.54
AFTER AGEING IN SOLAR BOX CHAMBER						
Silo N7 t=10s	149.37	150.17	155.46	149.81	160.33	153.94
Silo N7 t=60s	148.81	147.85	156.36	143.21	157.28	150.70
Rhodorsil H224 t=10s	145.84	137.76	157.80	149.42	143.72	146.91
Rhodorsil H224 t=60s	144.73	132.46	151.62	148.56	142.61	144.00
Fluoline HY t=10s	89.940	144.12	130.72	136.49	138.98	127.65
Fluoline HY t=60s	80.930	141.27	127.79	132.03	135.50	123.50

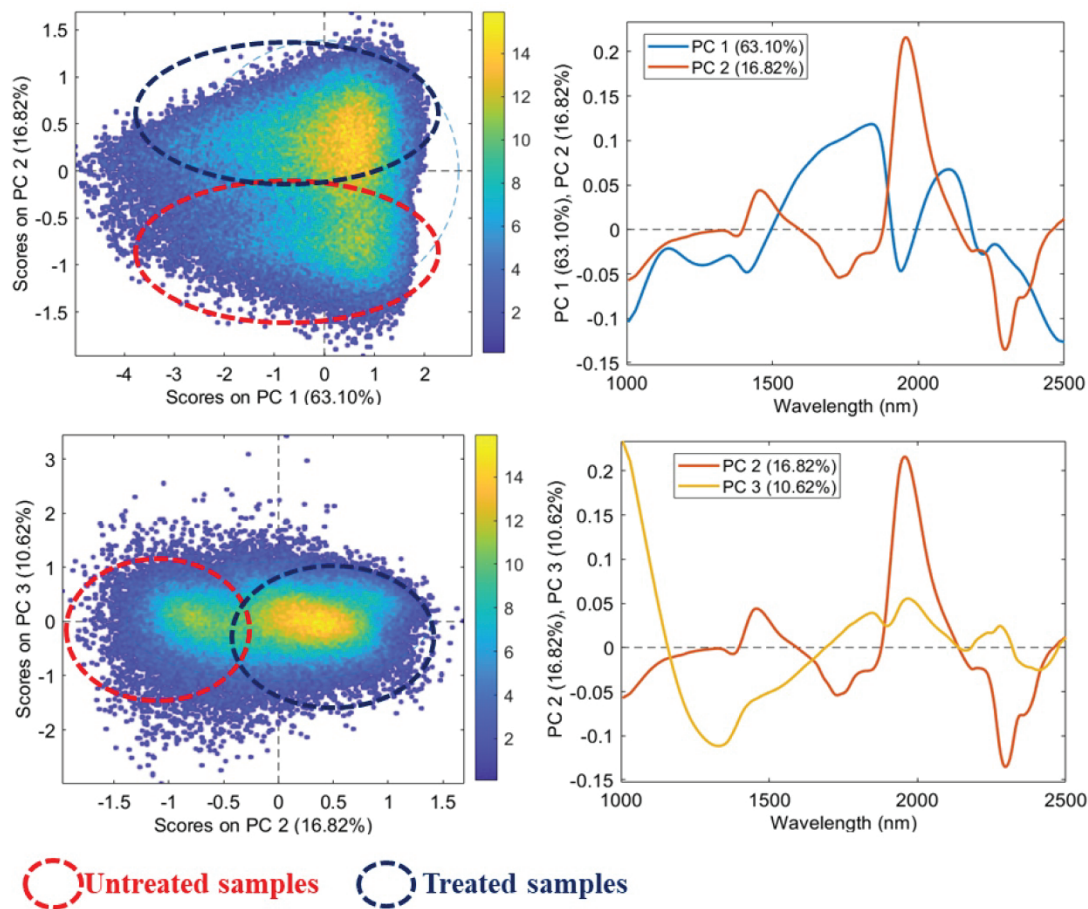


FIGURE 4. PCA score plot of the overall data obtained by HSI in the SWIR. In red circle untreated samples are differentiated in respect to the treated ones (blue circle).

The raw and preprocessed spectra of the Silo N7 treated samples and the corresponding PCA score and loadings plots are reported in Figure 5. The pre-processing combination selected 1 was MSC (median), Detrend, Mean Center (Fig. 5b). The results of PCA show that most of the variance was captured by the first four PCs, where PC1, PC2, PC3 and PC4 explained 70.77%, 14.22%, 8.29% and 2.09% of the variance, respectively. As shown in the PCA score plot (Fig. 5c), the spectral data of Silo N7 samples at T0 and T1000 and untreated samples at T0 and T1000 are clustered into two groups according to their spectral signatures that are samples untreated and treated with Silo N7. The positive values of PC2 (Figure 5d) for treated samples allows its separation from the untreated stones, while other PC score plot and relative loading plot does not allow a separation between samples at time 0h and same ones at time 1000h.

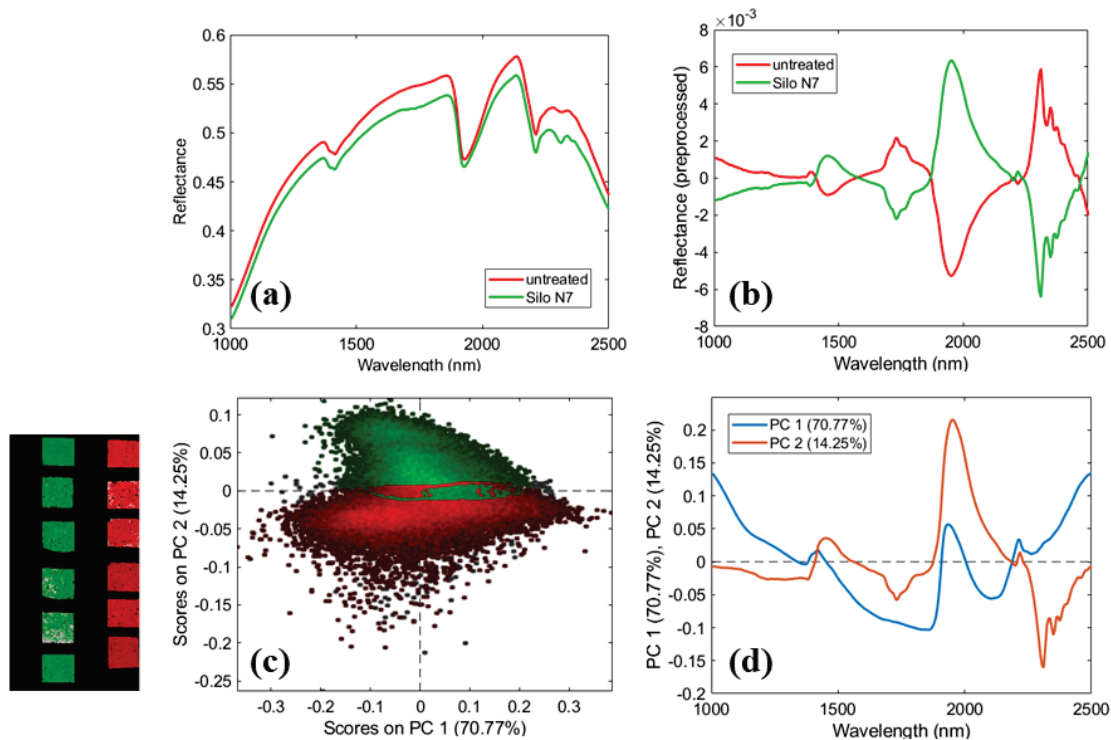


FIGURE 5. Average reflectance spectra acquired in the SWIR range (1000–2500 nm) (a), preprocessed average reflectance spectra (b), PCA score plot (c) and loadings plot (d) of PC1 and PC2 related to untreated and Silo N7 treated samples.

The raw and preprocessed spectra of the Rhodorsil H224 treated samples and the corresponding PCA score and loadings plots are reported in Figure 6. The pre-processing combination selected 1 was Detrend, SNV, Mean Center (Fig. 6b). The results of PCA indicated that most of the variance was captured by the first four PCs, where PC1, PC2, PC3 and PC4 explained 48.90%, 29.95%, 7.42% and 3.95% of the variance, respectively. As shown in the PCA score plot (Fig. 6c), the spectral data of Rhodorsil H224 treated samples at T0 and T1000 and untreated samples at T0 and T1000 are clustered into two groups according to their spectral signatures, i.e. samples untreated and treated with Rhodorsil H224. The positive values of PC2 (Figure 6d) for treated samples allows its separation from the untreated stones, while other PC score plot and relative loading plot does not allow a separation between samples at time 0h and same ones at time 1000h.

The raw and preprocessed spectra of the Fluoline HY treated samples and the corresponding PCA score and loadings plots are reported in Figure 7. The pre-processing combination selected 1 was Detrend, normalize (1-Norm, Area = 1), Mean Center (Fig. 7b). The results of PCA indicated as most of the variance was captured by the first four PCs, where PC1, PC2, PC3 and PC4 explained 48.85%, 25.32%, 8.82% and 5.09% of the variance, respectively. As shown in the PCA score plot (Fig. 7c), the spectral data of Fluoline HY treated samples and untreated samples at T0 and T1000 are clustered into two groups according to their spectral signatures, that is samples treated with Fluoline HY treated and untreated samples. The positive values of PC2 (Figure 7d) for treated samples allows its separation from the untreated stones while PC score plot and relative loading plot does not allow a separation between samples at time 0h and same samples at time 1000h.

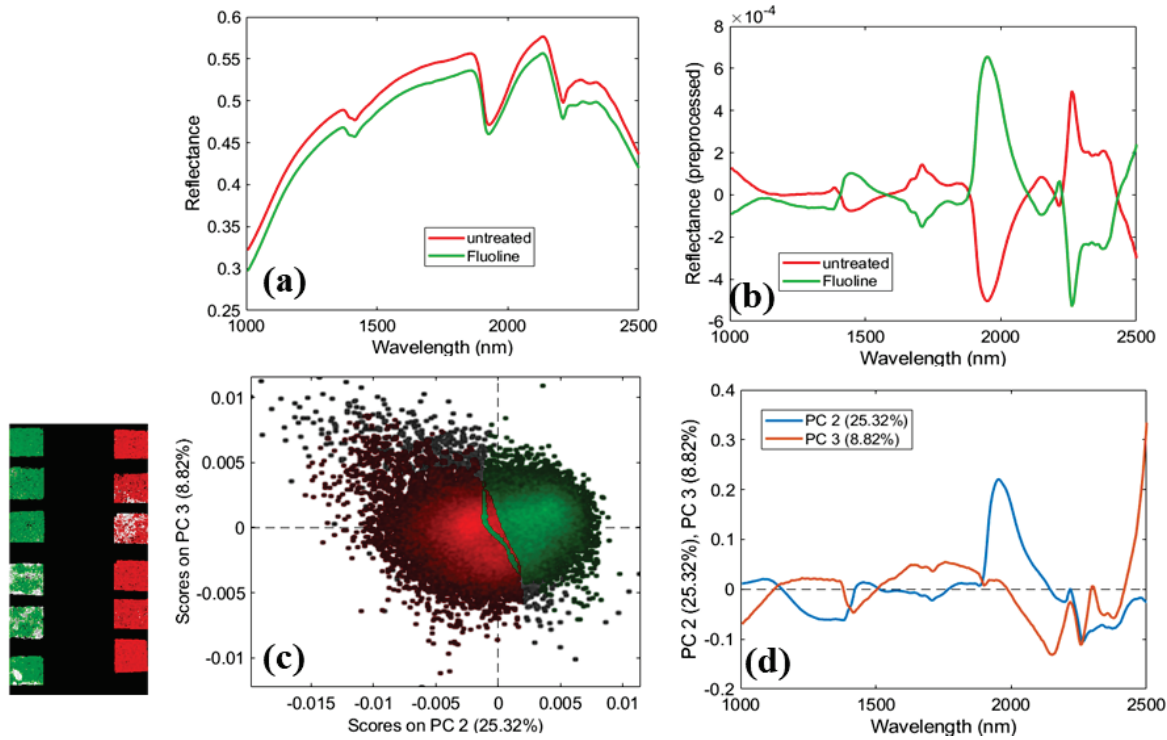


FIGURE 6. Average reflectance spectra acquired in the SWIR range (1000–2500 nm) (a), preprocessed average reflectance spectra (b), PCA score plot (c) and loadings plot (d) of PC2 and PC3 related to untreated and Fluoline HY treated samples.

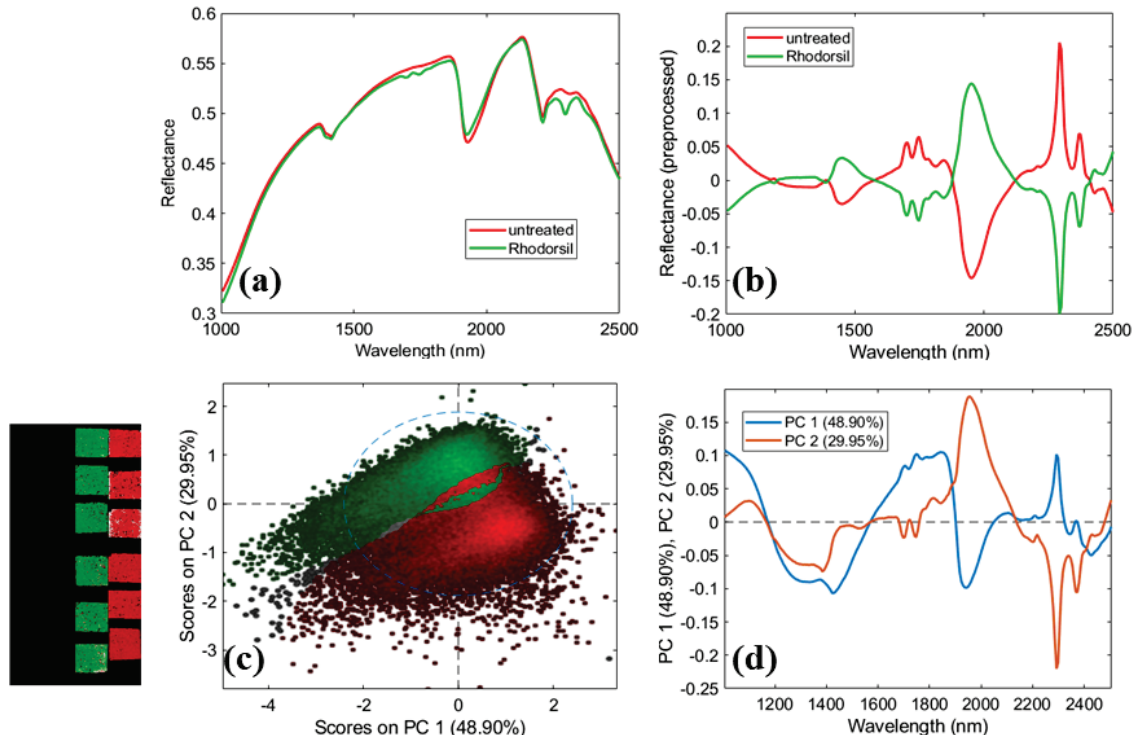


FIGURE 7. Average reflectance spectra acquired in the SWIR range (1000–2500 nm) (a), preprocessed average reflectance spectra (b), PCA score plot (c) and loadings plot (d) PC2 and PC3 related to untreated and Rhodorsil H224 treated samples.

CONCLUSIONS

A study was carried out to investigate the performance of three protective products applied on Sperone stone, a deposit of welded volcanic scoriae forming a portion of the Tuscolanio-Artemisio caldera rim, used for the construction of the fountains in Villa Mondragone, one of the site chosen for developing the activities of ADAMO project within the Center of Excellence Technological District of Cultural Heritage of Lazio Region.

Two selected products are commercial formulas based on poly-siloxane polymer and fluorinated elastomer respectively. The third one was a product, not yet on the market, kindly supplied by CTS for the tests; it is based on functionalized nano-silica.

The products were applied on the stone samples and their behaviour was evaluated according to the standard UNI EN16581:2016, by measuring colour, contact angle and capillarity absorption before and after ageing under controlled conditions.

Moreover, Hyperspectral Imaging, coupled with a chemometric approach, was also applied as a powerful, non-invasive, technique suitable to study the variations between samples. Colour measurements before and after the application of the protective products showed that in all cases the protective formula altered the stone surface colour causing a significant decrease of lightness (darkening of the stone). Silo N7 and Fluoline HY caused lower colour variation in respect to Rhodorsil H224. Colour measurements before and after the artificial ageing, both under UV irradiation and thermo-hygrometric cycles, showed that very little changes occurred for untreated and protective-treated samples. In all cases, the protective are stable towards the exposure to ageing factors.

This result is confirmed also by the contact angle measurements, which allow for assessing that in all cases the protective guarantee high hydrophobicity of the stone surfaces and that the ageing under simulated solar radiation doesn't significantly affect the behaviour of the products. The capillarity absorption test showed that Rhodorsil H224 is the most effective product in terms of increased hydrophobicity of the stone surface.

HSI coupled with chemometric approach allowed separating the treated from the untreated samples and confirming the low variation of protective layer from time 0h to time 1000h. This result was also underlined by colour, contact angle and capillarity adsorption measurements. It is important to stress that the proposed approach could be profitably applied, in the near future, thanks to the growing of HSI technologies and corresponding computing power, to perform, not only quality control, but also monitoring actions, in respect to treated areas with protective products. Future work will be addressed to strengthen the logics presented in this paper in an "in-situ" application perspective.

ACKNOWLEDGMENTS

This work was performed within the activities of ADAMO project funded by Lazio Region (Grant No. G06970, 30 May 2018). It is one of the projects of the Center of Excellence Technological District of Cultural Heritage of Lazio Region.

Special thanks are addressed to Dr. Leonardo Borgioli for having supplied the product Silo N7, not yet commercialized at the time of the experimental and so particularly suited for the tests. Now, after the testing phase, the product is marketed under the name of Nano Silo W.

Thanks to the restorers Maria Grazia Chilosi and Mark Gittins (CBC Society) for their suggestions and indications to choose the most suitable protective products.

REFERENCES

1. C. Cornaro, V. A. Puggioni, R. M. Strollo, [Journal of Building Engineering](#), **6**, 17-28 (2016).
2. F. Grossi Gondi, Di una villa dei Quintili nel Tuscolano, *Bullettino della Commissione Archeologica Comunale di Roma*, 1898.
3. A. Gentili, "La pietra "Sperone" di Villa Mondragone (Monte Porzio Catone - Roma): un caso di studio nell'ambito del progetto ADAMO del DTC Lazio", Master degree Thesis, University of Tuscia, 2020.
4. M. Fornaseri, A. Scherillo, U. Ventriglia, *La regione vulcanica dei Colli Albani: il Vulcano Laziale* (Consiglio Nazionale delle Ricerche Rome, 1963), 561 pp.
5. M. D. Jackson, F. Marra, R. L. Hay, C. Cawood, E. Winkler, [Archaeometry](#) **47**, 485–510 (2005).

6. UNI EN:17114, Conservation of cultural heritage - Surface protection for porous inorganic materials - Technical and chemical data sheets of water repellent product (Ente Italiano di Normazione, Milano, 2019).
7. C. D. Vacchiano, L. Incarnato, P. Scarfato, D. Acerno, *Construction and Building Materials* **22**, 855-865 (2008).
8. L. de Ferri, P. P. Lottici, A. Lorenzi, A. Montenero, E. Salvioli-Mariani, *J. Cult. Herit.* **12**, 356-363d (2011).
9. G. Cappelletti, P. Fermo, M. Camiloni, *Progress in Organic Coatings* **78**, 511-516 (2015).
10. D. Colangiuli, A. Calia, N. Bianco, *Construction and Building Materials* **93**, 189-196 (2015).
11. L. D'Orazio, A. Grippo, *Progress in Organic Coatings* **79**, 1-7 (2015).
12. L. D'Orazio, A. Grippo, *Progress in Organic Coatings* **99**, 412-419 (2016).
13. M. F. La Russa, S. A. Ruffolo, N. Rovella, C. M. Belfiore, P. Pogliani, C. Pelosi, M. Andaloro, G. M. Crisci, *Periodico di Mineralogia* **83**, 187-206 (2014).
14. A. Sierra-Fernandez, L.S. Gomez-Villalba, M.E. Rabanal, R. Fort, *Materiales de Construcción* **67**, e107 (2017).
15. L. D'Arienzo, P. Scarfato, L. Incarnato, *J. Cult. Herit.* **9**, 253-260 (2008).
16. UNI EN16581, Conservation of Cultural Heritage – Surface Protection for Porous Inorganic Materials – Laboratory Test Methods for the Evaluation of the Performance of Water Repellent Products (Ente Italiano di Normazione, Milano, 2016).
17. UNI EN15886, Conservation of Cultural Property-Test Methods — Colour Measurement of Surfaces (Ente Italiano di Normazione, Milano, 2010).
18. UNI EN15801, Conservation of cultural property - Test methods - Determination of water absorption by capillarity (Ente Italiano di Normazione, Milano, 2010).
19. UNI EN15802, Conservation of cultural property - Test methods - Determination of static contact angle (Ente Italiano di Normazione, Milano, 2010).
20. G. Bonifazi, S. Serranti, G. Capobianco, G. Agresti, L. Calienno, R. Picchio, C. Pelosi, *J. Electron. Imaging* **26**, 011003 (2016).
21. G. Bonifazi, G. Capobianco, C. Pelosi, S. Serranti, *Journal of Imaging* **5**, 1-19 (2019).
22. C. Pelosi, G. Capobianco, G. Agresti, G. Bonifazi, F. Morresi, S. Rossi, U. Santamaria, S. Serranti, *Spectroch. Acta A* **198**, 92-106 (2018).
23. G. Agresti, G. Bonifazi, G. Capobianco, L. Lanteri, C. Pelosi, S. Serranti, A. Veneri, Tattoo Wall: study of the stability of an innovative decorative technique through hyperspectral imaging and possible application in the mural painting's restoration, *Proc. SPIE 11058, Optics for Arts, Architecture, and Archaeology VII*, 110581G (12 July 2019); doi: 10.1117/12.2525726.
24. G. Agresti, G. Bonifazi, G. Capobianco, L. Lanteri, C. Pelosi, S. Serranti, A. Veneri, *Microch. J.* **157**, 104866 (2020).
25. H. Grahn, P. Geladi, P. (Eds.) *Techniques and Applications of Hyperspectral Image Analysis*, (JohnWiley & Sons, West Sussex, UK, 2007) pp. 1-15.
26. M. Otto, *Chemometrics, Statistics and Computer Application in Analytical Chemistry*, (Wiley-VCH, New York, 1999).
27. M. Vidal, J. M. Amigo, *Chemometr. Intell. Lab.* **117**, 138-148 (2012).
28. Å. Rinnan, F. van den Berg, S. B. Engelsen, *TrAC-Trend Anal. Chem.* **28**, 1201-1222 (2009).
29. J. M. Amigo, H. Babamoradi, S. Elcoroaristizabal, *Anal. Chim. Acta* **896**, 34-51 (2015).
30. Å. Rinnan, L. Nørgaard, F. van den Berg, J. Thygesen, R. Bro, S. B. Engelsen, "Data pre-processing", in *Infrared Spectroscopy for Food Quality Analysis and Control* (Academic Press, New York, 2009), Chapter 2, pp. 29-50.
31. R. Bro, A. K. Smilde, *Anal. Methods* **6**, 2812-2831 (2014).
32. G. Bonifazi, L. Calienno, G. Capobianco, A. Lo Monaco, C. Pelosi, R. Picchio, S. Serranti, *Polym. Degrad. Stab.* **113**, 10-21 (2015).
33. G. Bonifazi, L. Calienno, G. Capobianco, A. Lo Monaco, C. Pelosi, R. Picchio, S. Serranti, *Environl Sci. Pollut. R.* **24**, 13874-13884 (2017).